Journal of Applied Electrochemistry (2005) 35: 507–512
DOI 10.1007/s10800-005-0938-y

Li–H_2 cells with molten alkali chlorides electrolyte

HIROSHI ITO[1,*], YASUO HASEGAWA[1], and YASUHIKO ITO[2]
[1]*Energy Technology Research Institute, National Institute of Advanced Industrial Science and Technology, 1-2 Namiki, Tsukuba, 305-8564, Japan*
[2]*Department of Environmental Systems Science, Faculty of Engineering, Doshisha University, Kyotanabe-shi, Kyoto, 610-0321, Japan*
*(*author for correspondence, e-mail: ito.h@aist.go.jp)*

Received 27 February 2004; accepted in revised form 07 January 2005

Key words: electromotive force, lithium hydride, molten alkali chlorides, nickel membrane, thermally regenerative fuel cell

Abstract

Li–H_2 thermally regenerative fuel cells were studied using molten alkali chlorides as the electrolyte at relatively lower temperature. The saturation solubility of LiH in three different alkali chloride eutectic melts (LiCl–KCl, LiCl–CsCl, and LiCl–KCl–CsCl) was determined based on equilibrium potential measurements for the hydrogen electrode. Both a Ni membrane electrode and porous Ni electrode were evaluated as the cathode of the cell. In addition, a single cell of a Li–H_2 fuel cell with a Ni membrane for the anode was constructed, and the electromotive force (emf) was measured. When the Ni membrane electrode performed as an anode with molten salt electrolyte saturated with LiH, the measured emf was similar to previously reported emf for other types of molten salt electrolyte. In conclusion, certain types of molten alkali chlorides can be used as the electrolyte of a thermally regenerative fuel cell at a relatively lower operating temperature at least above 598 K.

1. Introduction

An electrochemical cell can be coupled with a high temperature heat source to decompose the products and regenerate the reactants of reaction. This system can be considered a direct energy conversion device that converts part of the heat energy absorbed at high temperature into electricity [1, 2]. Candidates for these thermally regenerative fuel cells depend on the type of active mass. A Li–H_2 thermally regenerative fuel cell system consists of the cell part and the regeneration part. The cell part is based on H_2 gas, molten salt electrolyte, and Li metal that reacts with the hydrogen, and the cell product LiH is then transported to the regeneration part. In the regeneration part, LiH is thermally decomposed to H_2 and Li. H_2 is returned to the cell cathode and Li is returned to the cell anode. This system can achieve a high Carnot cycle efficiency and low total weight, and thus shows promise as a power supply for both space and terrestrial applications [3, 4].

In our previous research into Li–H_2 cell development [5–9], molten alkali chlorides were used as the electrolyte due to their low corrosiveness, ease of handling, and a well-established method for purification. LiCl–KCl eutectic melt is a standard molten alkali chloride salt, and its thermophysical properties have been extensively measured [10–12]. Therefore, we have studied the electrochemical behavior of hydrogen reduction in LiCl–KCl melt, which is the cathode reaction in Li–H_2 cells, by using voltammetric analysis and ac impedance analysis with several types of electrode material [5, 6]. Results showed that hydrogen reduction occurred in this melt, and that Ni and Fe are the most suitable cathode materials due to their hydrogen solubility and stability. To achieve higher Carnot cycle efficiency in Li–H_2 cells, the electrolyte should be operated at lower temperature [1, 2]. When LiCl–KCl eutectic melt is used, the operating temperature is limited to above about 650 K, because the eutectic point of this melt is 625 K. There are several eutectic alkali chloride mixtures with melting points lower than that of LiCl–KCl eutectic melt [13, 14]. Among them, eutectic mixtures of LiCl–CsCl (mp = 596 K) and LiCl–KCl–CsCl (mp = 538 K), such as LiCl–KCl, are expected to be suitable for the electrolyte. We have measured the densities of LiCl–CsCl and LiCl–KCl–CsCl below 673 K by using the Archimedean method [7]. In the development of Li–H_2 cells, the behavior of hydride ions in molten alkali halide must be known, because these ions work as the charge carriers in the electrolyte. Therefore, the electrochemical behavior of hydride ions in LiCl–KCl, LiCl–CsCl, and LiCl–KCl–CsCl eutectic melts has been examined using voltammetric analysis [8]. The results showed that these three melts are promising candidates as the electrolyte of

Li–H_2 cells. Hydrogen reduction in LiCl–CsCl and LiCl–KCl–CsCl melts has been investigated at relatively lower temperatures below 673 K using the potential sweep method and ac impedance method in the same way as used to investigate hydrogen reduction in LiCl–KCl melt [9]. The hydrogen solubility and diffusion coefficient of hydrogen atoms in the metal electrode affected the voltammetric and impedance, behavior, in not only LiCl–KCl but also in LiCl–CsCl and LiCl–KCl–CsCl melts [9]. Based on these experimental results, LiCl–CsCl and LiCl–KCl–CsCl, which have lower operating temperatures, are possible candidates as the electrolyte of Li–H_2 cells.

Li–H_2 thermally regenerative fuel cell systems were extensively investigated in the 1950s and 1960s [15, 16], and the eutectic composition of alkali halide and LiH has been researched as part of the Li–H_2 cell development at the Argonne National Laboratory (ANL) [16]. ANL measured the emf of this cell in which the cathode was hydrogen passing through a porous metal and the anode was Li retained on a sintered metal sponge in several types of melt from 673 to 852 K [17]. Because the melting point of most of these melts was higher than that of LiCl–KCl eutectic melt, the cell was limited to a relatively higher operating temperature, above 673 K.

Formation of metal hydride in molten salt where hydride ions (H^-) are the hydrogen-transporting species was studied in the 1980s [18–21]. Those studies suggested that a metal membrane could be used for the anode of Li–H_2 fuel cells. Based on those results, in 1987 Roy et al. [22] proposed a Li–H_2 thermally regenerative fuel cell in which a thin hydrogen-permeable membrane was used as the anode. Figure 1 shows a schematic of the cell developed in the 1950s and the cell proposed by Roy et al. in 1987. Although Roy et al. showed (based on emf measurement) the effectiveness of the membrane anode in the cell [23], details of the experimental conditions were not reported.

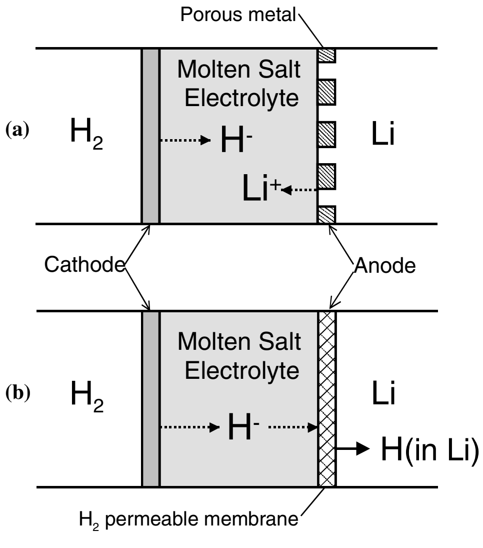

Fig. 1. Li–H_2 cell (a) developed in the 1950's and 60's and (b) proposed in 1987 by Roy et al. [22].

In this current study, the saturation solubility of Li–H_2 in molten alkali chlorides was measured to define general characteristics of molten alkali chlorides as the electrolyte in a Li–H_2 cell. In addition, emf was measured for a Li–H_2 cell that had a H_2 gas cathode, a Li anode, and molten alkali chloride electrolyte. Two types of electrode for the H_2 gas cathode were evaluated, namely, a porous Ni electrode, and a Ni membrane electrode with a closed-end Ni tube. The anode was another closed-end Ni tube containing Li. Three eutectic mixtures, LiCl–KCl, LiCl–CsCl and LiCl–KCl–CsCl, were evaluated as the electrolyte.

2. Experimental

The electrochemical cell was placed in a Pyrex container, which was hermetically sealed and connected to a glove box. Figure 2 shows a schematic of the experimental apparatus used for the emf measurement. The three eutectic mixtures, LiCl–KCl (58.8 + 41.2 mol%), LiCl–CsCl (59.3 + 40.7 mol%), and LiCl–KCl–CsCl (57.5 + 13.3 + 29.2 mol%), were prepared from anhydrous reagents that had been dried in a vacuum oven at 150 °C for more than two days. Each mixture was then put into an alumina crucible (Nikkato Co., SSA-S) and evacuated in a Pyrex container for two days at about 100 K below its respective melting point (i.e., at 573 K for LiCl–KCl, 473 K for LiCl–CsCl, 423 K for

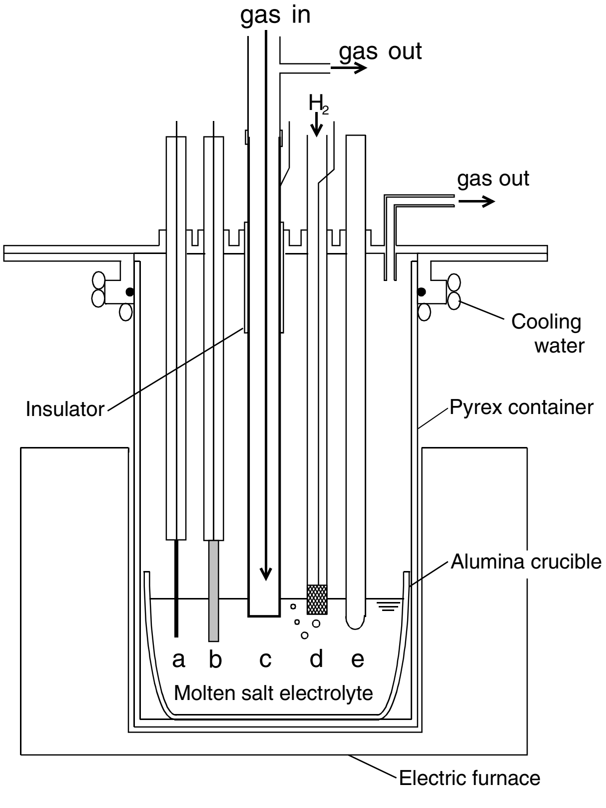

Fig. 2. Schematic of experimental apparatus used for potential measurement. (a) Li deposition electrode, (b) reference electrode (Li–Al alloy), (c) Ni membrane electrode, (d) porous Ni electrode, and (e) thermocouple.

LiCl–KCl–CsCl). Each mixture was then melted under an Ar atmosphere. The molten salt was evacuated again and purified by bubbling Ar through it. The condition of the melt and the electrodes inside the Pyrex container could be observed for brief periods of about 1 min during the experiments by lowering the furnace (Figure 2).

The rest potential was measured for two types of cathode. One was a porous electrode consisting of a tightly bound assembly of a Ni porous body (Celmet®#6, Sumitomo Electric Industries, Ltd.) within an outer alumina tube (4.0-mm inner diameter). The porous body for the passage of H_2 was 10 mm long with a specific surface of 5600 m^{-1}, and the bottom half was immersed in the melt. The other type was a hydrogen-permeable membrane electrode consisting of a closed-end Ni tube (6.0-mm outer diameter and 4.0-mm inner diameter). Another closed-end Ni membrane tube was also used as an anode by putting about 0.5 g of Li in the closed-end of the tube electrode; the resulting height of the melted Li was about 40 mm from the bottom of the tube. In the anode, about 10 mm of the bottom end of the tube was immersed in the molten salt electrolyte. Because the melting point of Li is 452 K, Li melted easily at the operating temperature of the cell, and the Ni membrane tube worked as an anode membrane. For both types of cathodes, the H_2 partial pressure of the cathode was adjusted by controlling the flow rates of H_2 and Ar, and the total flow rate was always maintained at 50 ml·min^{-1} at a total pressure of 1 atm. When the Ni membrane tube was used as a Li anode, liquid Li was exposed to an Ar atmosphere at 1 atm inside the tube. The placement/replacement of electrodes, addition of LiH into the melts, and filling the Ni tube with Li were all done in an inert atmosphere in a glove box. The temperature of the melts was measured using a chromel–alumel (type K) thermocouple sheathed in an alumina tube. High purity grade H_2 and Ar were used for the bubbling and the blanketing gas, respectively, after passing through a molecular sieve (5A) for purification. For both gases, the oxygen content was less than 0.1 ppm and the dew point was below −70 °C.

3. Results and discussion

3.1. *Porous Ni as a hydrogen cathode*

The rest potential of a hydrogen electrode as a function of concentration of hydride ions, H^- (i.e., added LiH) from 0.1 to 2.0 mol% was previously measured using a porous Ni electrode with three different eutectic melts, LiCl–KCl, LiCl–CsCl, and LiCl–KCl–CsCl, at 723, 673, and 623 K, respectively [8]. For all three melts, the rest potential vs. Li deposition potential (Li^+/Li) decreased linearly with increasing concentration of added LiH, and the slope of each line corresponded to the theoretical value, $= -2.303RT/F$, where R is the gas constant, T is temperature, and F is the Faraday constant. These results showed that LiH is soluble in these melts and is ionized to Li ions (Li^+) and hydride ions (H^-), and that the effect of decomposition by impurities in the melt is insignificant in this temperature range. In contrast, the potential shifted linearly to the positive direction with increasing H_2 gas pressure, and the slope corresponded to the theoretical value, $-2.303RT/2F$.

The Nernstian relationships indicate that the rest potentials measured in these three melts correspond to the equilibrium potential according to the reaction scheme:

$$H_2 + 2e^- \rightarrow 2H^- \tag{1}$$

Therefore, the equilibrium potential of the hydrogen electrode is given by the following Nernst equation:

$$E_{H_2} = E^0_{H_2} + \frac{RT}{2F}\ln\frac{p_{H_2}}{(a_{H^-})^2} \tag{2}$$

where $E^0_{H_2}$ denotes the standard electrode potential of this redox reaction, p_{H_2} is the partial pressure of H_2, and a_{H^-} is the activity of H^- ions in molten salt electrolyte.

In this study, to define the saturation solubility of LiH in molten alkali chloride, LiH was added until the melt was saturated. Then, the equilibrium potential of the hydrogen electrode was measured by using a porous Ni electrode in each of the three different eutectic melts (LiCl–KCl, LiCl–CsCl, and LiCl–KCl–CsCl). Figure 3 shows the measured rest potential of the hydrogen electrode as a function of concentration of added LiH at a constant H_2 pressure of 1 atm.

For LiCl–KCl, the rest potential reached a constant level when the LiH concentration was approximately 8.5 mol%. In this region, white precipitates were observed on the melt surface. These results confirmed that a constant rest potential is an indicator that the LiCl–KCl eutectic melt was saturated with LiH. Based on this indicator, the LiCl–CsCl and LiCl–KCl–CsCl

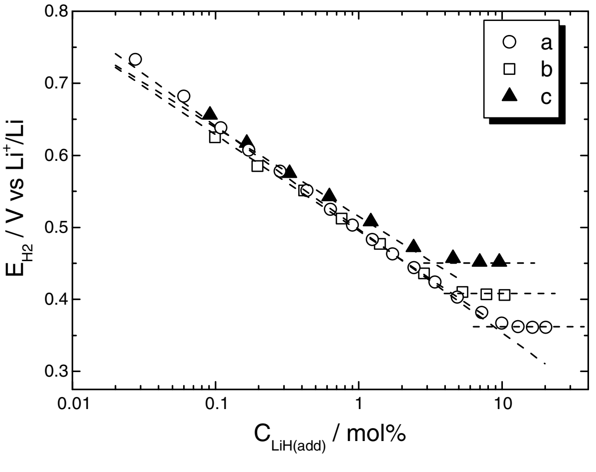

Fig. 3. Rest potential of a porous Ni cathode vs. added LiH concentration under constant hydrogen pressure of 1 atm for eutectic melts of (a) LiCl–KCl at 723 K, (b) LiCl–CsCl at 673 K, and (c) LiCl–KCl–CsCl at 623 K. Dashed lines show theoretical slope calculated from $-2.303RT/F$.

Table 1. Saturation solubility of LiH in molten alkali chlorides

Melt composition (m/o)	Temperature (K)	Saturation solubility of LiH (mol%)
LiCl–KCl (58.8–41.2)	723	8.5 ± 0.3
LiCl–CsCl (59.3–40.7)	673	4.6 ± 0.3
LiCl–KCl–CsCl (57.5–13.3–29.2)	623	3.2 ± 0.3

eutectic melts were saturated when the LiH concentration was 4.6 mol% at 673 K and 3.2 mol% at 623 K, respectively (Table 1). At these respective saturation conditions and temperature, the rest potential of the hydrogen electrode vs. Li^+/Li was about 0.36 V in the LiCl–KCl melt, 0.41 V in LiCl–CsCl melt, and 0.45 V in LiCl–KCl–CsCl melt.

3.2. *Ni membrane as a hydrogen-permeable cathode*

To confirm the applicability of the membrane electrode as the cathode, a closed-end tube electrode made of pure Ni was used for the hydrogen cathode. Based on previous research on hydrogen reduction [5, 6, 9], Ni was chosen as the membrane electrode material due to its high hydrogen-permeability, high corrosion-resistance, and machinability. About 10 mm of the bottom end of the closed-end of the tube was immersed in the melt.

Figure 4 shows the rest potential of the Ni membrane electrode in LiCl–KCl eutectic melt at 723 K as a function of added LiH concentration. In the added LiH concentration region from 0.2 to 1.0 mol%, the potential measured for the Ni membrane electrode was similar to that for the porous Ni electrode (Figure 3), and the slope of the measured potential agreed well with the theoretical slope calculated from the Nernst equation (Equation (2)). In contrast, when the added LiH concentration was below 0.1 mol% or above 2.0 mol%, the potential of the Ni membrane electrode differed from that of the porous Ni electrode. This difference in potential at the low LiH concentration cannot yet be definitively explained. The difference in potential at high LiH concentration, however, might be due to some LiH adhering to the surface of the Ni membrane tube before saturation of the electrolyte, because the temperature of that part of the tube might be lower than the surrounding temperature.

When the melt was saturated with LiH (i.e., above 8.5 mol% LiH), the rest potential of the Ni membrane electrode (Figure 4) was similar to that of the porous Ni electrode (Figure 3), which was about 0.36 V vs. Li^+/Li. Figure 5 shows that the rest potential of the Ni membrane electrode in LiCl–KCl melt as a function of hydrogen partial pressure p_{H_2} yielded a straight line, where the slope corresponded to the theoretical value ($=-2.303RT/2F$) in the p_{H_2} range from 1.0 to 0.6 atm.

The rest potential measurement results for the Ni membrane electrode (Figures 4 and 5) show that this type of electrode could be used as the cathode in molten chloride electrolyte. Because the current–potential characteristics have not yet been studied for either the Ni membrane electrode or the porous Ni electrode, the suitability of either of these electrodes as the cathode cannot be definitively determined. However, one advantage of using the membrane electrode as the cathode is that optimum shapes can be fabricated relatively easily.

3.3. *Ni membrane as a Li anode*

In a Li–H_2 cell with a porous metal anode developed in the 1950s and 60s [15, 16], the following anode reaction progresses as shown in Figure 1(a) [3]:

$$\mathrm{Li}(\ell) \rightarrow \mathrm{Li}^+(\text{in electrolyte}) + \mathrm{e}^- \tag{3}$$

H^-ions and Li^+ ions in molten salt electrolyte are transported to the thermal regeneration part of the cell

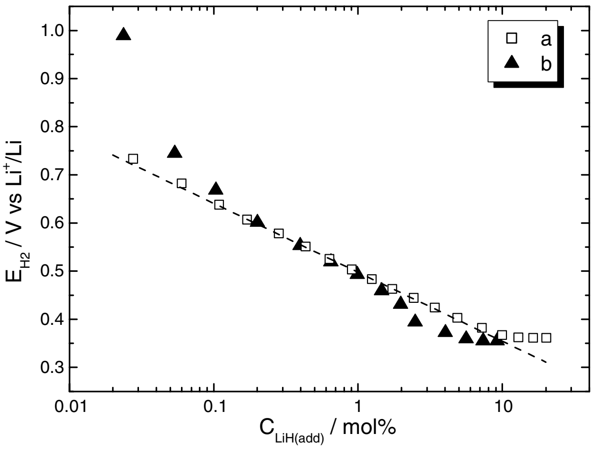

Fig. 4. Rest potential of hydrogen electrode for (a) porous Ni electrode and (b) Ni membrane electrode in LiCl–KCl eutectic melt at 723 K. Dashed line shows theoretical slope calculated from $-2.303RT/F$.

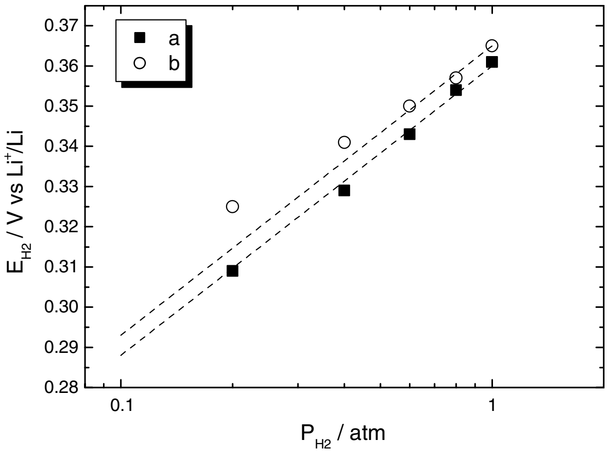

Fig. 5. Rest potential of hydrogen electrode vs. hydrogen partial pressure for (a) porous Ni in LiCl–KCl eutectic melt at 723 K containing 20.2 mol% LiH, and (b) Ni membrane electrode in LiCl–KCl eutectic melt at 723 K containing 9.2 mol% LiH. Dashed lines show theoretical slope calculated from $-2.303RT/2F$.

immediately before saturation of the electrolyte and formation of LiH in the electrolyte. In a Li–H_2 cell with a hydrogen-permeable membrane anode proposed Roy et al. [22, 23], the following anode reaction is expected as shown in Figure 1(b):

$$H^- \rightarrow H(\text{in liquid Li}) + e^- \qquad (4)$$

First, H^- ions dissolved in the melt diffuse to the anode and then oxidize into hydrogen atoms (H). Then, these H atoms diffuse to the other side of the membrane anode, and dissolve in liquid Li. The equilibrium potential of this anode (E_a) is given by the following Nernst equation:

$$E_a = E_a^0 + \frac{RT}{F}\ln\frac{a_H}{a_{H^-}} \qquad (5)$$

where E_{a^0} denotes the standard electrode potential of this redox reaction, a_H is the activity of H in liquid Li, and a_{H^-} is the activity of H^- in molten salt electrolyte. The emf (ΔE) of this cell can be written as follows by considering the cathode potential:

$$\Delta E = E^0 + \frac{RT}{F}\ln\frac{(p_{H_2})^{1/2}}{a_H} \qquad (6)$$

where E^0 is the standard emf calculated from the Gibbs energy. Pure H_2 gas at 1 atm pressure was chosen as the standard state. Then, substituting $p_{H_2} = 1$ for H_2 pressure of 1 atm, the emf at a given temperature can be determined by E^0 and a_H.

To clarify the effectiveness of the Li–H_2 cell proposed by Roy et al. (Figure 1(b)), the potential of the anode using a hydrogen-permeable membrane was measured in this current study. The Ni membrane electrode used for the hydrogen cathode can also be used as a membrane anode, that is, a Ni membrane tube electrode filled with Li and immersed in the melt.

Figure 6 shows the rest potential of the Li anode in LiCl–KCl eutectic melt at 723 K as a function of concentration of LiH added to the electrolyte, and shows the cathode potential of the hydrogen electrode with Ni porous body at $p_{H_2} = 1$ atm. The measured emf of the cell (i.e., the potential difference between the cathode and anode) was far smaller than the emf reported in the literature [17]. The reason for this disagreement between measured and theoretical emf is due to the anode potential being more positive than expected. Although emf data measured at the standard state was about 0.35 V at this temperature (723 K) [17], the emf measured here ranged from 0.05 to 0.125 V. The reason for this disagreement in emf is that the wettability of Li to Ni inside the Ni membrane was insufficient for the Ni membrane to function as the anode.

When a Ni membrane was used for the anode, with increasing operating temperature, the anode potential rapidly shifted to the negative side, finally reaching a constant when the temperature exceeded about 800 K. When the temperature was then decreased, the anode potential did not return to its original value, but was always equal to the potential of the Li deposition electrode (Li^+/Li) at a given temperature. One explanation for this hysteresis in the potential is that the wettability of Li to Ni was improved by increasing the temperature, that is, the Ni membrane performed properly as an anode. Another explanation is that liquid Li dissolved in Ni, resulting in the α-solid solution of Li being formed in the Ni matrix, thus enabling contact between α-Li in Ni and the melt.

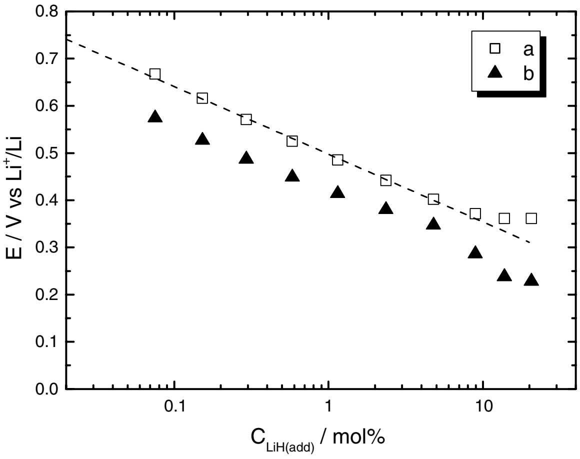

Fig. 6. Rest potential for a (a) hydrogen cathode and (b) Li anode in LiCl–KCl eutectic melt at 723 K. Dashed line shows theoretical slope calculated from $-2.303RT/F$.

Johnson et al. [17] measured the emf for a cathode in which H_2 passed though a porous metal and the anode in which Li was retained on a sintered metal sponge in several types of melt from 673 to 852 K. In the present study, when the melts were saturated with LiH after the wettability at the anode had been improved by increasing the temperature, the measured emf and its temperature dependence agreed well with that reported by Johnson et al. [17], regardless of the type of melt, as shown in Figure 7. Each potential was measured by using the hydrogen cathode with a porous Ni body (under constant pressure of 1 atm) and the Li anode of Ni tube in the three different eutectic melts saturated with LiH.

The solubility of hydrogen in liquid Li was determined by Adams et al. [24], who reported the following empirical formula for the solubility as a function of temperature in the range 523 to 775 K:

$$\log x_H = 1.523 - \frac{2308}{T} \qquad (7)$$

where x_H is the solute mole fraction of H. In the temperature range 598 to 723 K, the calculated solubility ranges 0.5 to 3.4 mol% of H. Johnson et al. [17] measured the emf at the standard state (i.e., pure

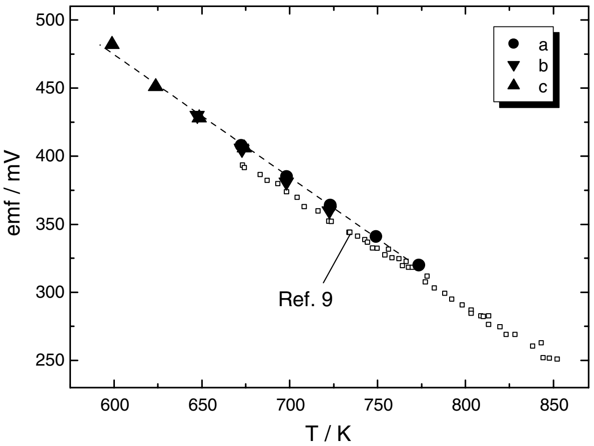

Fig. 7. Temperature dependence of measured emf for cell with eutectic melt of (a) LiCl–KCl at 723 K containing 16.7 mol% LiH, (b) LiCl–CsCl at 673 K containing 8.8 mol% LiH, and (c) LiCl–KCl–CsCl at 623 K containing 11.2 mol% LiH. Dashed line shows fitted line, and white squares show reference data obtained by Johnson et al. [17].

hydrogen gas of 1 atm and solid LiH precipitated in the electrolyte). In this study, the state of H_2 gas of 1 atm and H saturated in liquid Li could be chosen as the standard state based on Equation (6). Because the solubility of hydrogen in liquid Li is small, H might have been saturated in liquid Li at the temperature range studied here. Therefore, the measured emf in this study agrees well with that reported by Johnson et al. [17].

In conclusion, the emf at operating temperature lower than 673 K was measured by using molten alkali chloride electrolyte with low melting point, and the linear relationship between the operating temperature and emf is extensible to temperatures at least above 598K.

4. Summary

In this study of Li–H_2 cells, molten alkali chlorides were used for the electrolyte due to their low corrosiveness, ease of handling and well-established method for purification. The saturation solubility of LiH in three different alkali chloride eutectic melts was determined based on equilibrium potential measurements for the hydrogen electrode of a Li–H_2 cell. Both a Ni membrane electrode and a porous Ni electrode were evaluated as cathode. In addition, a single cell of a Li–H_2 fuel cell using a Ni membrane for the anode was constructed, and the emf was measured. When the Ni membrane electrode performed properly as an anode with molten salt electrolyte saturated with LiH, the measured emf was similar to that previously reported for other types of molten salt electrolyte. In conclusion, certain types of molten alkali chlorides, such as not only LiCl–KCl but also LiCl–CsCl and LiCl–KCl–CsCl eutectic melts, can be used as the electrolyte of a thermally regenerative fuel cell at a relatively lower operating temperature at least above 598 K.

References

1. R. Roberts, *J. Electrochem. Soc.* **105** (1958) 428.
2. A.J. deBethne, *J. Electrochem. Soc.* **107** (1960) 937.
3. T.A. Ciarlariello and R.C. Werner, *Chem. Eng. Prog.* **57** (1961) 42.
4. D.R. Snoke and J.M. Fuscoe, *SAE J.* **69** (1961) 68.
5. H. Ito and Y. Hasegawa, *J. Electrochem. Soc.* **147** (2000) 289.
6. H. Ito, Y. Hasegawa and Y. Ito, *J. Electrochem. Soc.* **148** (2001) E148.
7. H. Ito, Y. Hasegawa and Y. Ito, *J. Chem. Eng. Data* **46** (2001) 1203.
8. H. Ito, Y. Hasegawa and Y. Ito, *J. Electrochem. Soc.* **149** (2002) E273.
9. H. Ito, Y. Hasegawa and Y. Ito, *J. Electrochem. Soc.* **150** (2003) E244.
10. E.R. Van Artsdalen and I.S. Yaffe, *J. Phys. Chem.* **59** (1955) 118.
11. Y. Matsumura, Y. Tanaka and M. Mizuno, *Trans. Jpn. Welding Soc.* **4** (1973) 126.
12. D.A. Nissen and R.W. Carlsten, *J. Chem. Eng. Data* **18** (1973) 75.
13. G.J. Janz, 'Molten Salt Handbook' (Academic Press, New York, 1967).
14. E.J. Cairns and K. Steunenberg, in C.A. Rouse (Ed.), 'Progress in High Temperature Physics and Chemistry', vol. 5, Chap. 2 (Pergamon Press, Oxford, 1972).
15. H.L. Chum and R.A. Osteryoung, 'Review of Thermally Regenerative Electrochemical Systems', vol. 2, SERI-TR-332-416 (Solar Energy Research Institute, Golden ,CO, 1980).
16. E.J. Cairns, C.E. Crouthamel, A.K. Fisher, M.S. Foster, J.C. Hesson, C.E. Johnson, H. Simotake and A.D. Tevebaugh, 'Galvanic cells with fused salt electrolytes' 'Chemical Engineering Division', Report No. ANL-7316 (Argonne National Laboratory, 1967).
17. C.E. Johnson, R.R. Heinrich and C.E. Crouthamel, *J. Phys. Chem.* **70** (1966) 242.
18. C.M. Luedecke, G. Deblein and R.A. Huggins, *J. Electrochem. Soc.* **132** (1985) 52.
19. C.M. Lüdecke, G. Deublein and R.A. Huggins, *Int. J. Hydrogen Energy* **12** (1987) 81.
20. B.Y. Liaw and R.A. Huggins, *Z. Physik. Chem. N. F.* **164** (1989) 1533.
21. B.Y. Liaw. Hydride-containing molten salts and their technology implications, in C.A.C. Sequeira and G.S. Picard (Eds), Electrochemical Technology of Molten Salt 1-2, (Trans Tech Publications, Switzerland, 1993), pp. 345–357.
22. R. Roy, J.S. Armijo and E.E. Gerrels, 'Proceedings of the 23rd IECEC', vol. 2 (Denver, CO, 1988) pp. 287.
23. R. Roy, S.A. Salamah, J. Maldonado and R.S. Narkiewicz, 'A.I.P. Conference Proceedings', vol. 271, Part 2 (Albuquerque, NM, 1992) pp. 913.
24. P.F. Adams, M.G. Down, P. Hubberstey and R.J. Pulham, *J. Less-Common Metals* **42** (1975) 325.